

# Characterizing Interfacial Roughness by Light Scattering Ellipsometry

Thomas A. Germer

*Optical Technology Division, National Institute of Standards and Technology,  
Gaithersburg, Maryland 20899*

The polarization of light scattered by oxide films thermally grown on photolithographically-generated microrough silicon surfaces was measured as functions of scattering angle. Using the predictions of first-order vector perturbation theory for scattering from interfacial roughness to interpret the results, the roughness of each interface and the correlation function between the two interfaces can be determined. The results show the spatial frequency dependence of the SiO<sub>2</sub>/Si interface smoothing. The impact of these results on the inspection of silicon wafers with dielectric films is discussed.

## 1. INTRODUCTION

Interfacial roughness is a concern to a variety of issues in the development of ultra-large scale integrated devices. For example, roughness of a SiO<sub>2</sub>/Si interface at a gate oxide affects dielectric breakdown and the transport properties of carriers in the silicon.<sup>1</sup> The scattering of light by interfacial roughness often limits the sensitivity of optically-based defect inspection tools.<sup>2</sup> Roughness also contributes to uncertainties in the metrology of film thickness and line widths. Despite the importance of roughness in the performance of dielectric films and coatings, *in situ* measurement of the morphology of each of the two interfaces of a film has been difficult. X-ray and neutron scattering measurements can be used to determine roughness parameters, but the analyses require extensive modeling, with the results being model dependent.<sup>3-5</sup> Spectroscopic ellipsometry is often used to determine interfacial roughness, but is limited to extracting an effective interfacial width.<sup>6-8</sup> Atomic force microscopy (AFM) is capable of measuring only the exposed interface of a material, requiring that buried interfaces be initially exposed.<sup>9-11</sup>

Recent work has demonstrated that the polarization of scattered light contains information that allows the source of scattering, be it surface roughness, subsurface defects, or particulate contamination, to be identified.<sup>12-15</sup> In particular, it was found that the polarization of light scattered by a single rough interface does not lead to depolarization. This finding led to the development of microroughness-blind instrumentation, enhancing the sensitivity of light scatter tools to defects and particles in the presence of a background dominated by roughness. Improvements in sensitivity to small defects of a factor of approximately two in feature

diameter were shown to be possible with such techniques.<sup>16</sup>

When light scattering tools are used to detect small features in dielectric films, the background signal originates from roughness of two interfaces. In order to develop roughness-blind instrumentation for such materials, the sources of light scattering from rough dielectric layers must be understood.

In this article, measurements of the intensity and polarization of light elastically scattered from rough dielectric layers are reported. These measurements demonstrate that ellipsometry, a commonly used technique for measuring film thickness, can be extended to the scattering regime, yielding film roughness and cross-correlation statistics. The only parameters required for the analysis are the optical constants of the substrate and film and the thickness of the film, which can be extracted from data obtained in the specular condition. Therefore, light scattering ellipsometry enables a complete non-contact, non-destructive characterization of the roughness of both interfaces.

## 2. THEORY

It is widely known that the intensity of light elastically scattered by a bare surface in the smooth surface limit is proportional to the power spectral density (PSD) function,  $|Z(\mathbf{q})|^2$ , of the surface height  $z(x,y)$ .<sup>17</sup> When the only source of scattering is variation of the height of the surface, when those surface height variations are small compared to the wavelength of the light, and when the surface slopes are much less than unity, first-order vector perturbation theory predicts that the differential Stokes-vector power scattered into a specific direction, defined by polar angle  $\theta_r$  and azimuthal (out-of-plane) angle  $\phi_r$ , is given by<sup>18,19</sup>

$$d\mathbf{P}_s = (16\pi^2 / \lambda^4) \cos \theta_i \cos^2 \theta_r |Z(\mathbf{q})|^2 \mathbf{Q} \cdot \mathbf{P}_i d\Omega, \quad (1)$$

where  $\theta_i$  is the incident polar angle,  $Z(\mathbf{q})$  is the two-dimensional Fourier transform of  $z(x,y)$ ,  $\mathbf{P}_i$  is the incident Stokes-vector power,  $d\Omega$  is the differential solid angle of collection, and  $\mathbf{Q} = \mathbf{Q}(\theta_i, \theta_r, \phi_r)$  is a Mueller matrix, which depends upon the optical constants of the surrounding media and converges to the sample reflectance matrix when  $\theta_i = \theta_r$  and  $\phi_r = 0$  (the specular condition). The Fourier transform is evaluated at a surface wavevector  $\mathbf{q}$ , whose components are determined by the Bragg condition:

$$\begin{aligned} q_x &= k(\sin \theta_i \cos \phi_r - \sin \theta_r) \\ q_y &= k \sin \theta_r \sin \phi_r \end{aligned} \quad (2)$$

where  $k = 2\pi/\lambda$ . Eqs. (1) and (2) are used to extract surface roughness from angle-resolved scattering data over the entire electromagnetic spectrum.

The first-order vector perturbation theory has been extended to allow for multiple interfaces.<sup>20-22</sup> The extended theory predicts a dependence of the scattering on the PSDs of each interface and the degree of phase correlation between the interfaces. Measurements have been performed on optical multilayers demonstrating application of the theory in the limits of high or low correlation.<sup>23-25</sup> These studies have primarily relied on the presence or absence of interference features in the angular distribution of intensity that exist due to the interference of the fields scattered from each interface and only exist for optically thick films or multilayers. Angle-resolved light scattering at three different wavelengths has been employed to characterize a single dielectric layer, but it was found that not enough information is available to extract the roughness of each interface and the cross-correlation statistics.<sup>26</sup>

For example, measurements testing the consistency of the polarization with the matrix  $\mathbf{Q}$  can be used to validate the use of Eqs. (1) and (2).<sup>12-14</sup> The vector perturbation theory for light scattering from a rough dielectric film predicts a polarization dependence to the light scattering, which, like the amplitude, depends upon the roughness of each interface and the correlation between the interfaces. Calculations for the polarization of light scattered by the interfaces of a dielectric film have been performed for optical multilayers, and these results have been compared to experimental data in specific limits.<sup>27</sup> The author, however, knows of no case where the roughness parameters have been extracted from experimental data.

The scattering from the  $i$ -th interface can be calculated using first-order vector perturbation theory,<sup>21</sup> yielding a scattered electric field  $\mathbf{A}_i Z_i$ , where  $\mathbf{A}_i$  is a complex (Jones) vector, and  $Z_i$  is the Fourier transform of the surface height function, evaluated at the surface

vector  $\mathbf{q}$  given by Eq. (2). The vector  $\mathbf{A}_i$  depends upon the film thickness, the optical constants of the film and substrate, the wavelength, the incident polarization, and the scattering geometry. The Stokes vector power  $\mathbf{P}_s$  describing the net scattering from both interfaces is then given by

$$\mathbf{P}_s = \mathbf{S}(\mathbf{A}_1 Z_1 + \mathbf{A}_2 Z_2), \quad (3)$$

where  $\mathbf{S}(\mathbf{X})$  is the Stokes vector representation of the Jones vector  $\mathbf{X}$ . If we let  $Z_2 = \chi Z_1$ , and assume  $C \equiv \langle \chi / |\chi| \rangle$  is real, then Eq. (3) can be written as

$$\mathbf{P}_s = \{(1-C)[\mathbf{S}(\mathbf{A}_1) + \mathbf{S}(|\chi| \mathbf{A}_2)] + C\mathbf{S}(\mathbf{A}_1 + |\chi| \mathbf{A}_2)\} |Z_1|^2. \quad (4)$$

Eq. (4) indicates that the ratio of the magnitudes of the interfacial roughness,  $|\chi|$ , and the degree of phase correlation between the interfaces,  $C$ , determine the polarization state of the scattered light. As long as no degeneracies exist, the measurable polarization can be inverted to yield these parameters.

### 3. EXPERIMENT

The samples used in this study consisted of two microfabricated silicon wafers, each having a pseudorandom distribution of two diameters of circular shallow pits (nominal diameters of 1.31  $\mu\text{m}$  and 1.76  $\mu\text{m}$ , depths of 8 nm, and density of  $8 \times 10^4 \text{ mm}^{-2}$ ). Oxide layers were thermally grown on each of these wafers with thicknesses of 10.3 nm and 52 nm, respectively, as determined by specular ellipsometry. The roughnesses of the two interfaces on each sample are expected to be coherent and identical, at least for small  $\mathbf{q}$ . A previous study showed that the polarization of light scattered by similar samples before growth of the oxide layers was consistent with scattering from microroughness.<sup>12-14</sup>

Light of wavelength  $\lambda$  (633 nm, 532 nm, 442 nm, or 325 nm) was incident onto each sample at an angle of  $\theta_i$  (45°, 60°, or 68°). Light scattered into a solid angle  $d\Omega$  ( $1.39 \times 10^{-4}$  sr or  $2.87 \times 10^{-6}$  sr) defined by a polar angle of  $\theta_r$  ( $= \theta_i$ ) and azimuthal angle  $\phi_r$  is analyzed as a function of  $\phi_r$ . The incident light is linearly-polarized at an angle given by  $\eta_i = \pi/4 + \phi_r/2$ , with respect to  $s$ -polarization. The out-of-plane geometry with  $\eta_i = \pi/2$  ( $p$ -polarized) has been shown to maximize the differentiation between different scattering mechanisms at  $\phi_r = \pi/2$ .<sup>12-14</sup> By employing  $\eta_i = \pi/4$  for  $\phi_r = 0$ ,  $\eta_i = 3\pi/4$  for  $\phi_r = \pi$ , and continuously varying between these limits, we improve the differentiation for a wider range of  $\phi_r$ . The polarization of the scattered light is measured by rotating a quarter-wave retarder, followed by a linear polarizer, in front of the detector. A detailed description of the instrument can be found elsewhere.<sup>28</sup>

## 4. RESULTS

Figure 1 shows a representative measurement of polarization parameters as functions of  $\phi_r$ . The polarizations are represented by the principal angle that the polarization ellipse makes with respect to  $s$  polarization,  $\eta$ , the degree of circular polarization,  $P_C$ , and the degree of polarization,  $P$ . It is straightforward to show that these parameters fully describe the polarization and map onto the usual Stokes parameters. The uncertainties in the data are dominated by statistical sources and are thus similar to the point-to-point variation observable in the data.

Curves (a)—(d) shown in Fig. 1 show the predicted behavior for the four limiting cases of correlated and equal roughness ( $|\chi| = 1$ ,  $C = 1$ ), uncorrelated but equal roughness ( $|\chi| = 1$ ,  $C = 0$ ), bottom interface roughness ( $\lim |\chi| \rightarrow \infty$ ), and top interface roughness ( $|\chi| = 0$ ). Only for the case of uncorrelated roughness is any depolarization predicted. While the data follow the correlated and equal roughness model for small angles ( $\phi_r < 10^\circ$ ), they deviate significantly for higher angles.

The parameters  $\eta$ ,  $P_C$ , and  $P$  are fit to Eq. (4), letting  $|\chi|$  and  $C$  be adjustable parameters, constrained to be in the ranges  $(0, \infty)$  and  $(-1, 1)$ , respectively. The resulting fits follow very close to the data shown in

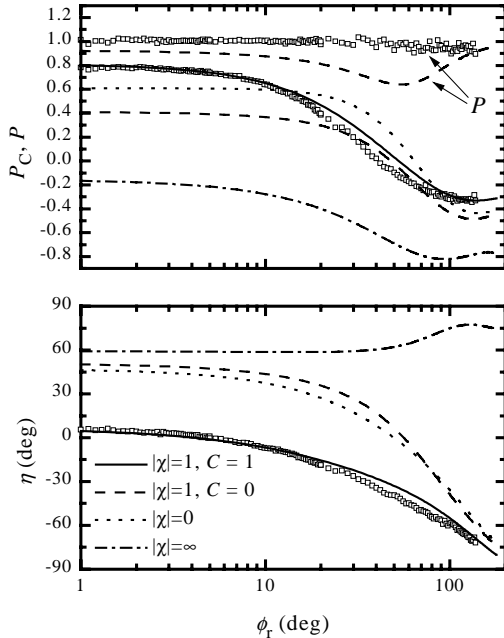


FIG. 1 Polarization of scattered light [(top)  $P_C$  and  $P$ , and (bottom)  $\eta$ ] measured for the 52 nm  $\text{SiO}_2$  film on Si, using  $\lambda = 532$  nm, and  $\theta_i = \theta_r = 68^\circ$ . The curves represent the theory in four different limits. The theory for  $C = 1$  predicts  $P = 1$ .

Fig. 1. Figure 2 shows  $|\chi|$  and  $C$  extracted from the fits for both samples using measurements taken with  $\lambda = 532$  nm and  $\theta_i = \theta_r = 45^\circ, 60^\circ$ , and  $68^\circ$ . The 90 % confidence limit uncertainties in both extracted parameters are approximately 0.04, or the point-to-point fluctuations in the data, whichever is larger. Fits obtained with measurements at 325 nm, 442 nm, and 633 nm are consistent with those shown in Fig. 2. The agreement between the different wavelengths and incident angles suggests that the analysis is valid.

For both the 10.3 nm and the 52 nm oxide samples, the two interfaces appear to be highly correlated ( $C \sim 1$ ) and, for small periodicities ( $|\mathbf{q}|/2\pi < 0.5 \mu\text{m}^{-1}$ ), the two surfaces have equal amplitudes ( $|\chi| \sim 1$ ). As previously mentioned, the oxidation process should be uniform on long length scales. The 10.3 nm oxide sample shows this high degree of conformity for all the periodicities probed. On the other hand, the 52 nm oxide sample shows a noticeable deviation of  $|\chi| > 1$ , indicating either roughening of the top interface or smoothing of the buried interface. This mismatched amplitude does not follow any features in the degree of correlation between the two surfaces.

Once the parameters  $|\chi|$  and  $C$  are extracted from the polarization data, Eq. (4) allows the intensity of the scattered light to be immediately converted to the PSD ( $|Z_i|^2$ ) of each interface. Figure 3 shows the resulting

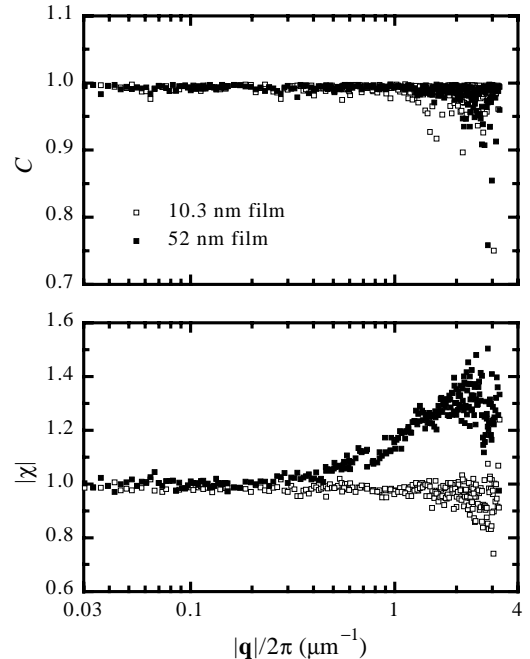


FIG. 2 Cross-interface roughness parameters,  $|\chi|$  and  $C$ , extracted from the measurements using  $\lambda = 532$  nm and  $\theta_i = \theta_r = 45^\circ, 60^\circ$ , and  $68^\circ$ . Symbols represent results for the (open) 10.3 nm film and (closed) 52 nm film.

PSDs for the 52 nm film measured with  $\lambda = 532$  nm. The results for the 10.3 nm film are similar on the scale shown, except that both interfaces are nearly identical. The curve shown in Fig. 3 shows the results of a calculation of the scattering from a random distribution of the two circular pits having their nominal diameters and

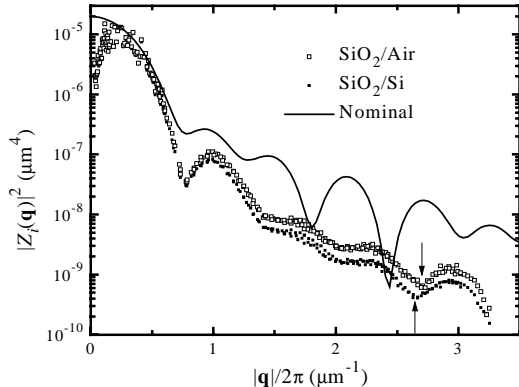


FIG. 3 The power spectral density function of each interface of the 52 nm film extracted from the amplitude of scattering. The curve represents the ideal case of two randomly-placed circular pits having their nominal diameters. The arrows point to a local minimum whose location is different for the two interfaces.

density, and shows structure resulting from two Airy diffraction patterns. The imperfect match between the experimentally measured PSDs and the nominal curve may be combined results from the lithography process that produced the structure (causing the actual diameters of the pits to differ from their nominal values), their pseudorandom distribution on the surface (one of each diameter, non-overlapping, per  $5 \mu\text{m} \times 5 \mu\text{m}$  square on the surface), and the film growth process. Aside from the smoothly varying differences between the two interfaces, the data in Fig. 3 also show a shift in a local minimum near  $2.7 \mu\text{m}^{-1}$ , which is near the fourth zero of the diffraction from the  $1.76 \mu\text{m}$  pits and the third zero from the  $1.31 \mu\text{m}$  pits. Other small shifts can be observed as derivative-like features in Fig. 2 near  $0.7 \mu\text{m}^{-1}$  and  $1.4 \mu\text{m}^{-1}$ . These shifts are a result of the pits in the buried interface having a larger diameter than those of the exposed interface. The presence of this shift suggests that the response function  $\chi(\mathbf{q})$  is a function of the interfacial roughnesses  $Z_i(\mathbf{q})$ , so that a linear response theory<sup>29</sup> would not completely describe the smoothening process.

## 5. DISCUSSION

Interfacial smoothening associated with the growth of  $\text{SiO}_2$  has been measured in the past, using atomic

force microscopy (AFM) and destructive removal of the oxide,<sup>9–11</sup> by spectroscopic ellipsometry,<sup>6–8</sup> and by x-ray scattering.<sup>3–5</sup> While AFM probes length scales much shorter than those presented in this work, it cannot measure the degree of correlation between the interfaces and cannot discern the level of relative roughness variation obtainable by the light scattering ellipsometry method. The spectroscopic ellipsometry measurements are only sensitive to interfacial widths, which are affected by roughness as well as the suboxide transition region. The x-ray measurements were performed in a manner which is also sensitive only to the interfacial width. The results of the AFM and x-ray studies, however, qualitatively agree with those presented here: the buried interface is smoother than the top interface, and the smoothness of the buried interface increases with thicker layers.

The ability to remove the background light scattering signal from a rough dielectric layer is determined by the degree of conformity between the two interfaces. It can be seen from Fig. 1 that for the 52 nm film, if the interfaces were randomly correlated, the degree of polarization would have a minimum of approximately 66% in the geometry shown. Detectors placed at that minimum, having polarizers aligned to maximally reduce the signal would only reduce the light scattering background by 66%. Due to the approximately  $d^6$  dependence on particle diameter of a particle's scattering cross section, the reduction in minimal detectable particle size would only be improved by about 7%.

In general, however, the case of uncorrelated but equal roughness is not likely to occur, and it is difficult to evaluate the discrimination that one would obtain without prior knowledge of the representative behaviors of the roughness PSDs for both interfaces. Furthermore, the scattering polarization depends upon the thickness of the dielectric film. Tools employing polarization analysis, therefore, must be able to adaptively change their polarization sensitivity depending upon the particular sample conditions encountered. Only in this way will such instruments find full versatility for detecting defects on silicon wafers with deposited dielectric films.

Roughness-blind operation can always be attained for a single interface of a dielectric stack. Light scattered by a single rough interface is always polarized, provided the film thicknesses remain constant. If a film is grown on a rough silicon surface followed by chemical-mechanical planarization (CMP), the quality of the polishing can be inspected.

## 6. SUMMARY

In this article, we have presented an ellipsometric scattering measurement for a dielectric film. The results demonstrate that these measurements permit a simulta-

neous measurement of the roughness of two interfaces and the correlation between the two interfaces, without requiring contact with the sample. This technique should prove valuable for studying the growth or deposition morphology for a variety of transparent films on surfaces.

## ACKNOWLEDGMENTS

The author would like to thank Bradley Scheer of VLSI Standards, Inc.<sup>30</sup> for providing the samples.

## REFERENCES AND NOTES

1. T. Ohmi, M. Miyashita, M. Itano, T. Imaoka, and I. Kawanabe, *IEEE Trans. Electron Device* **39**, 537 (1992).
2. J. C. Stover, *Optical Scattering: Measurement and Analysis*, (SPIE Optical Engineering Press, Bellingham, WA, 1995).
3. J. L. Dawson, K. Krisch, K. W. Evans-Lutterodt, M.-T. Tang, L. Manchanda, M. L. Green, D. Brasen, G. S. Higashi, and T. Boone, *J. Appl. Phys.* **77**, 4746 (1995).
4. M.-T. Tang, K. W. Evans-Lutterodt, G. S. Higashi, and T. Boone, *Appl. Phys. Lett.* **62**, 3144 (1993).
5. M.-T. Tang, K. W. Evans-Lutterodt, M. L. Green, D. Brasen, K. Krisch, L. Manchanda, G. S. Higashi, and T. Boone, *Appl. Phys. Lett.* **64**, 748 (1994).
6. V. A. Yakovlev and E. A. Irene, *J. Electrochem. Soc.* **139**, 1450 (1992).
7. V. A. Yakovlev, Q. Liu, and E. A. Irene, *J. Vac. Sci. Technol. A* **10**, 427 (1992).
8. C. Zhao, P. R. Lefebvre, and E. A. Irene, *Thin Solid Films* **313-314**, 286 (1998).
9. S. J. Fang, W. Chen, T. Yamanaka, and C. R. Helms, *J. Electrochem. Soc.* **144**, 2886 (1997).
10. L. Lai and E. A. Irene, *J. Appl. Phys.* **86**, 1729 (1999).
11. Q. Liu, L. Spanos, C. Zhao, and E. A. Irene, *J. Vac. Sci. Technol. A* **13**, 1977 (1995).
12. T. A. Germer, C. C. Asmail, and B. W. Scheer, *Opt. Lett.* **22**, 1284 (1997).
13. T. A. Germer, *Appl. Opt.* **36**, 8798 (1997).
14. T. A. Germer and C. C. Asmail, *J. Opt. Soc. Am. A* **16**, 1326 (1999).
15. L. Sung, G. W. Mulholland, and T. A. Germer, *Opt. Lett.* **24**, 866 (1999).
16. T. A. Germer, *Proc. AIP* **449**, 815 (1998).
17. P. Beckmann and A. Spizzichino, *The Scattering of Electromagnetic Waves from Rough Surfaces*, (Pergamon, Oxford, 1963).
18. D. E. Barrick, *Radar Cross Section Handbook* (Plenum, New York, 1970) Chap. 9.
19. S. O. Rice, *Comm. Pure and Appl. Math.* **4**, 351 (1951).
20. J. M. Elson, *J. Opt. Soc. Am.* **66**, 682 (1976).
21. J. M. Elson, *J. Opt. Soc. Am. A* **12**, 729 (1995).
22. E. Kröger and E. Kretschmann, *Z. Physik* **237**, 1 (1970).
23. C. Amra, *Appl. Opt.* **32**, 5481 (1993).
24. C. Amra, J. H. Apfel, and E. Pelletier, *Appl. Opt.* **31**, 3134 (1992).
25. C. Amra, C. Grèzes-Besset, and L. Bruel, *Appl. Opt.* **32**, 5492 (1993).
26. D. Rönnow, *Opt. Eng.* **37**, 696 (1998).
27. C. Deumiè, H. Giovannini, and C. Amra, *Appl. Opt.* **35**, 5600 (1996).
28. T. A. Germer and C. C. Asmail, *Rev. Sci. Instr.* **70**, 3688 (1999).
29. M. O. Robbins, D. Andelman, and J.-F. Joanny, *Phys. Rev. A* **43**, 4344 (1991).
30. Certain commercial equipment, instruments, or materials are identified in this paper in order to specify the experimental procedure adequately. Such identification is not intended to imply recommendation or endorsement by the National Institute of Standards and Technology, nor is it intended to imply that the materials or equipment identified are necessarily the best available for the purpose.